Published in final edited form as:
Exp Physiol. 2013 March ; 98(3): 679–691. doi:10.1113/expphysiol.2012.069377.

Bradycardic effects mediated by activation of G protein-coupled estrogen receptor (GPER) in rat nucleus ambiguus

G. Cristina Brailoiu[1], **Jeffrey B. Arterburn**[2], **Tudor I. Oprea**[3], **Vineet C. Chitravanshi**[4], and **Eugen Brailoiu**[5]

[1]Department of Pharmaceutical Sciences, Jefferson School of Pharmacy, Thomas Jefferson University, Philadelphia, PA 19140

[2]Department of Chemistry and Biochemistry, New Mexico State University, Las Cruces, NM 88003

[3]Translational Informatics Division, Department of Internal Medicine, University of New Mexico School of Medicine, Albuquerque, NM 87131

[4]Neurological Surgery, New Jersey Medical School, University of Medicine and Dentistry of New Jersey, Newark, NJ 07103

[5]Center for Translational Medicine, Temple University School of Medicine, Philadelphia, PA 19140

Abstract

G protein-coupled estrogen receptor (GPER) has been identified in several brain regions including cholinergic neurons of nucleus ambiguus, which are critical for the parasympathetic cardiac regulation. Using calcium imaging and electrophysiological techniques, microinjection into nucleus ambiguus and blood pressure measurement we examined the *in vitro* and *in vivo* effects of GPER activation in nucleus ambiguus neurons. G-1, a GPER selective agonist, produced a sustained increase in cytosolic Ca^{2+} concentration in a concentration-dependent manner in retrogradely-labeled cardiac vagal neurons of nucleus ambiguus. The increase in cytosolic Ca^{2+} produced by G-1 was abolished by pretreatment with G36, a GPER antagonist. G-1 depolarized cultured cardiac vagal neurons of nucleus ambiguus. The excitatory effect of G-1 was also identified by whole-cell visual patch-clamp recordings in nucleus ambiguus neurons, in medullary slices. To validate the physiological relevance of our *in vitro* studies, we carried out *in vivo* experiments. Microinjection of G-1 into the nucleus ambiguus elicited a decrease in heart rate; the effect was blocked by prior microinjection of G36. Systemic injection of G-1, in addition to a previously reported decrease in blood pressure, also reduced the heart rate. The G-1-induced bradycardia was prevented by systemic injection of atropine, a muscarinic antagonist, or by bilateral microinjection of G36 into the nucleus ambiguus. Our results indicate that GPER-mediated bradycardia occurs via activation of cardiac parasympathetic neurons of the nucleus ambiguus and support the involvement of GPER in the modulation of cardiac vagal tone.

Keywords

calcium; electrophysiology; vagus

Address correspondence to Vineet C. Chitravanshi (chitrava@umdnj.edu). Corresponding author: Eugen Brailoiu, M.D., Center for Translational Medicine, Temple University School of Medicine 3500 N. Broad Street, Philadelphia, PA 19140, Tel: 215-707-2791, ebrailou@temple.edu.

Introduction

Clinical and experimental observations indicate gender-related differences in autonomic regulation (Dart et al., 2002). With respect to the cardiovascular system, estrogen modulates autonomic functions by increasing vagal tone and/or decreasing sympathetic drive (Mercuro et al., 2000; Liu et al., 2003; Saleh and Connell, 2007; Weissman et al., 2009). Premenopausal women or postmenopausal women with estrogen replacement therapy have lower heart rate, increased baroreceptor sensitivity, and elevated heart rate variability (Huikuri et al., 1996, Virtanen et al., 2000). Experimental studies also indicate that systemic or central administration of estrogen increases parasympathetic tone and baroreflex sensitivity in rodents (Du et al., 1995; Mohamed et al., 1999; Saleh and Connell, 1999, 2000; Saleh et al., 2000a).

Increasing evidence support a role for G protein-coupled estrogen receptor 1 (GPER) in estrogen-mediated fast signaling. In addition to interacting with two classical nuclear receptors, ERα and ERβ and their extranuclear variants, estrogen has been shown to activate a G protein-coupled estrogen receptor 1 (GPER) (for review Prossnitz and Barton, 2011). We previously detected GPER immunoreactivity (irGPER) in many areas of the rat brain including the hypothalamus, nucleus of the solitary tract and nucleus ambiguus (Brailoiu et al., 2007), which are involved in autonomic homeostasis. The activity of the heart is controlled by a tonic level of parasympathetic activity that originates within the medulla, mainly in the nucleus ambiguus (Mendelowitz, 1999).

The detection of GPER immunoreactivity in the nucleus ambiguus (Brailoiu et al., 2007) prompted us to explore *in vitro* and *in vivo* effects of GPER activation in cardiac-projecting nucleus ambiguus neurons.

Materials and Methods

Ethical information

Experimental protocols were reviewed and approved by the Institutional Animal Care and Use Committee from Temple University and UNDMJ - New Jersey Medical School and were in accordance with the National Institute of Health Guide for the Care and Use of Laboratory Animals. All efforts were made to minimize the number of animals used and their suffering.

Drugs

The GPER agonist, G-1, (Bologa et al., 2007) and the GPER antagonist G36 (Dennis et al., 2011) were synthesized and provided by Dr. Jeffrey B. Arterburn. G-1 and G36 were dissolved in DMSO (stock solution 10^{-2} M), and frozen in aliquots. Shortly before administration, G-1 and G36 were thawed and dissolved in physiological saline to the desired concentration. Other drugs (atropine, urethane, L-glutamate) were from Sigma-Aldrich (Saint Louis, MO), unless otherwise mentioned.

Animals

Adult male Wistar rats were used for heart rate and blood pressure monitoring and microinjections into nucleus ambiguus, and neonatal rats (1–3-day-old) of either sex for calcium and voltage imaging and electrophysiology studies.

Neuronal culture

Cardiac vagal preganglionic neurons of nucleus ambiguus were retrogradely labeled by intrapericardial injection of rhodamine (X-rhodamine 5,6 isothiocyanate. X-RITC,

Invitrogen, Carlsbad, CA), similar to previous reports (Bouairi et al., 2006; Brailoiu et al., 2012). Rhodamine (0.01 %, 40 μl) was injected using a Hamilton syringe in the pericardial sac of 1–2-day-old rats, in the second intercostal space, on the right side of the sternum. Medullary neurons were dissociated and cultured 24 hours after rhodamine injection, as previously described (Brailoiu et al., 2009, 2012). The neuronal labeling was verified by fluorescence microscopy (excitation/emission= 520/560 nm) in medullary slices (300 μm thick), cut with a vibratome, fixed in paraformaldehyde, treated with DMSO and mounted in Citifluor. For the neuronal culture, the brains were quickly removed and immersed in ice-cold Hanks balanced salt solution (Mediatech, Manassas, VA). The ventral side of the medulla (containing nucleus ambiguus) was dissected, minced and the cells were dissociated by enzymatic digestion with papain, followed by mechanical trituration. After centrifugation at 500 x *g*, fractions enriched in neurons were collected and resuspended in Neurobasal-A medium (Invitrogen) containing 2 mM glutamine, 100 units/ml penicillin G, 100 μg/ml streptomycin and 10% fetal bovine serum (Atlanta Biologicals, Lawrenceville, GA). Cells were plated on round 25-mm glass coverslips in 6-well plates. Cultures were maintained at 37°C in a humidified atmosphere with 5% CO_2.

Measurement of cytosolic calcium concentration ($[Ca^{2+}]_i$)

$[Ca^{2+}]_i$ was measured by the calcium imaging technique, as previously described (Brailoiu et al., 2009, 2010a, 2012). Cultured neurons were incubated with 5 μM fura-2 AM (Invitrogen) in Hanks' balanced salt solution (HBSS) at room temperature for 45 min, in the dark, washed three times with dye-free HBSS, and then incubated for another 45 min to allow for complete de-esterification of the dye. Cells on coverslips were subsequently mounted in an open bath chamber (Warner Instruments, Hamden, CT) on the stage of an inverted microscope Nikon Eclipse TiE (Nikon Inc., Melville, NY) equipped with a Perfect Focus System and a Photometrics CoolSnap HQ2 CCD camera (Photometrics, Tucson, AZ). During the experiments the Perfect Focus System was activated. Fura-2 AM fluorescence (emission = 510 nm), following alternate excitation at 340 and 380 nm, was acquired at a frequency of 0.25 Hz. Images were acquired and analyzed using NIS-Elements AR 3.1 software (Nikon Inc.). The ratio of the fluorescence signals (F340/F380 nm) was converted to Ca^{2+} concentrations as described (Grynkiewicz et al., 1985).

Optical imaging using $DiBAC_4(3)$

Bis-oxonol (bis-[1,3-dibutylbarbituric acid] trimethineoxonol [$DiBAC_4(3)$], a slow-response voltage-sensitive fluorescent dye, has been successfully used to assess relative changes in membrane potential of single cells (Ebner and Chen, 1995). The method was similar to that previously described (Brailoiu et al. 2008, 2010b). Briefly, cells were incubated for 30 min in HBSS containing 0.5 mM $DiBAC_4(3)$. The fluorescence (excitation wavelength = 480 nm, emission wavelength = 540 nm) was continuously recorded at a rate of 10 points min^{-1}. Background values (windows of identical area placed besides the cells) were subtracted. The dye partition between the cell membrane and the cytosol is a function of membrane potentials. Depolarization of the membrane leads to a sequestration of the dye into cytosol and is associated with an increase in fluorescence intensity; whereas, the dye concentrates in the cell membrane during hyperpolarization, leading to a decrease of fluorescence intensity (Brauner et al. 1984). Calibration of $DiBAC_4(3)$ fluorescence was performed using the Na^+-K^+ ionophore gramicidin in Na^+-free physiological solution (Brauner et al. 1984).

Electrophysiology

Visual patch-clamp recordings were made from neurons of the nucleus ambiguus in neonatal rat medullary slices as previously described (Brailoiu et al., 2009). Neonatal rats were decapitated and the hindbrain dissected and placed in ice-cold Krebs solution of following composition (in mM): 127 NaCl, 1.9 KCl, 1.2 KH_2PO_4, 2.4 $CaCl_2$, 1.3 $MgCl_2$, 26 $NaHCO_3$,

and 10 glucose, oxygenated with 95% O_2 and 5% CO_2. Brainstem slices of 200 μm thickness were prepared using a vibratome. Slices were transferred to the recording chamber and superfused with oxygenated Krebs solution at a rate of 1 ml/min. Recordings were conducted at room temperature (20 ± 1°C) from neurons in the ventral perimeter of nucleus ambiguus previously identified as cardiac vagal neurons (Bouairi et al., 2006, Brailoiu et al., 2012). Patch electrodes pulled from thin-walled borosilicate glass capillaries were filled with a solution containing (in mM): 130 K gluconate, 1 $MgCl_2$, 2 $CaCl_2$, 4 ATP, 0.3 GTP, 10 EGTA and 10 HEPES, and had a resistance of 2–5 MΩ; the pH of the solution was adjusted to 7.2. Signals were recorded using an Axopatch 1C amplifier (Axon Instruments/ Molecular Devices, Sunnyvale, CA) and a Digidata 1320 digitizer in voltage- or current-clamp mode, filtered at 2 KHz, displayed on a two-channel Gould chart recorder RS 3200. Experimental protocols were controlled and data acquired by a personal computer using the Clampex 8.0 software (Axon Instruments). Steady-state current-voltage (IV) relationships of G-1-induced currents were investigated in rat nucleus ambiguus neurons voltage-clamped to −60 mV, which is close to the resting membrane potential of these neurons. Current-voltage relationships were obtained by applying a series of 400 ms voltage command steps every 5 s from a holding potential of −60 mV to potentials varying from −140 to 0 mV, with 10 mV increments, before and during the superfusion of G-1. Currents elicited by each voltage command step in control media were subtracted from their counterparts in the presence of G-1 to yield a steady-state IV curve of G-1-induced currents.

Microinjections in nucleus ambiguus

The procedures were similar to those described earlier (Chitravanshi and Sapru, 2011). Briefly, the rats were anesthetized with inhalation of isoflurane (2–3 % in 100 % oxygen), the trachea was cannulated, and the rats were artificially ventilated. One of the femoral veins was cannulated, and urethane was injected intravenously in 3–4 administrations with a volume of 200 μl each, at 2–4 min interval; the total dose was 1.2–1.4 g/kg. Rectal temperature was maintained at 36.5 ± 0.5°C. One of the femoral arteries was cannulated, and PAP, MAP and HR were measured using a 1401 A/D converter and Spike 2 software (Cambridge Electronic Design, Cambridge, UK) and the data was stored on a computer hard drive. The rats were placed in a prone position in a stereotaxic instrument with bite bar 18 mm below the interaural line. The microinjections were made using a dorsal approach. Four-barreled glass micropipettes (tip size 20–40 μm) were mounted on a micromanipulator, and each barrel was connected to one of the channels on a picospritzer. One barrel was filled with L-glutamate (L-Glu, 5 mM), the second barrel filled with DMSO 0.1% (vehicle for G-1), the third barrel was filled with G-1 (10 μM), and the fourth barrel was filled with G36 (10 μM). The following coordinates were used for the identification of the nucleus ambiguus: 0.3 caudal to 1.1 mm rostral and 1.8–2.0 mm lateral to the calamus scriptorius and 2.0–2.4 mm deep from the dorsal medullary surface; stimulation of this site has been shown to elicit the most prominent bradycardic response. The correct placement of the pipette assembly was determined by evaluating the bradycardic response to glutamate (5 mM, 30 nl). The volumes were pressure ejected (30–35 psi) and visually confirmed by the displacement of fluid meniscus in the barrel containing the solution. The duration of microinjection was 5–10 s.

Histology

Typical sites of microinjections in the nucleus ambiguus were marked by microinjections of diluted (1: 42) green Lumafluor retrobeads (Lumafluor Inc, Durham, NC). The animals were perfused and fixed with 4% paraformaldehyde, serial sections of the medulla were cut (30–40 μm), mounted on slides, covered with Vectashield mounting medium (Vector Laboratories, Burlingame, CA) and coverslipped. The microinjection sites were identified,

using a fluorescence microscope, photographed and compared with a standard rat brain atlas (Paxinos & Watson, 1998).

Statistical analysis

Data was expressed as means ± standard error of mean (SEM). In calcium and voltage imaging studies, and electrophysiological experiments, one-way ANOVA followed by post-hoc analysis using Bonferonni and Tukey tests was used to evaluate significant differences between groups; $P < 0.05$ was considered statistically significant. For comparison of HR responses, the mean and SEM were calculated for maximum changes in HR in response to microinjections of L-Glu or G-1 into the nucleus ambiguus. In the experiments testing for tachyphylaxis, comparisons of the maximum decreases in HR in different groups of rats were made using one-way ANOVA followed by Tukey-Kramer's multiple comparison.

Results

Activation of GPER increases $[Ca^{2+}]_i$ in cultured preganglionic neurons

Cardiac vagal neurons of nucleus ambiguus were labeled with rhodamine, a reliable marker for retrograde labeling (Bouairi et al., 2006; Brailoiu et al., 2012). Cultured neurons labeled with rhodamine were selected for calcium measurements (Fig. 1). G-1 (1 μM), a GPER agonist (Bologa et al. 2006), produced an increase in F340/F380 fluorescence ratio of Fura-2AM-loaded neurons (Fig. 1A); the effect was prevented by pretreatment with G36, a GPER antagonist (Fig. 1B). G-1 (1 μM) produced a transient increase in $[Ca^{2+}]$; the effect started 5–6 min after the G-1 treatment; a representative example is illustrated in Fig. 1C. Administration of G-1 (10 nM, 100 nM and 1 μM) produced dose-dependent increase in $[Ca^{2+}]_i$ by 6 ± 1.4 nM, 508 ± 4.1, and 914 ± 7.3 nM, respectively; n = 6 neurons for each concentration tested (Fig. 1D). In neurons pretreated with the GPER antagonist G36 (1 μM), G-1 (1 μM) increased $[Ca^{2+}]_i$ by only 47 ± 2.4 nM (n = 6) (Fig. 1C, D).

Activation of GPER depolarizes cultured cardiac vagal neurons of nucleus ambiguus

The effect of G-1 on the membrane potential of rhodamine-labeled cardiac vagal neurons was tested by voltage imaging in neurons loaded with the slow-response voltage-sensitive fluorescent dye, $DiBAC_4(3)$. G-1 depolarized retrogradely labelled nucleus ambiguus neurons in a dose-dependent manner: G-1 (10 nM, 100 nM and 1 μM) produced a depolarization with an amplitude of 1.6 ± 0.2, 9.7 ± 0.3, and 14.2 ± 0.5 mV, respectively; n = 6 neurons for each concentration tested (Fig. 2A–B). The G-1-induced depolarization was abolished by pretreatment with G36 (1 μM); the average amplitude of the depolarization induced by G-1 (1 μM) in neurons pretreated with G36 (1 μM) was 0.8 ± 0.2 mV (n = 6) (Fig. 2A, B).

Activation of GPER depolarizes nucleus ambiguus neurons in medullary slices

Nucleus ambiguus neurons were visually identified via DIC illumination in the ventrolateral quadrant of the medullary slice. The mean resting membrane potential and input resistance of nucleus ambiguus neurons were −55.1 ± 1.4 mV and 692 ± 39.2 MΩ, respectively (n = 72). Nucleus ambiguus neurons were generally silent, and injection of depolarizing currents (50 – 100 pA, 300 ms) elicited repetitive firings followed by a hyperpolarization (Fig. 2C), as previously reported (Mendelowitz, 1996). G-1 (10 nM) produced an increase in firing activity with little change in membrane potential; an example is shown in Fig. 2D (top trace). At higher concentrations, G-1 (100 nM and 1 μM) depolarized the neurons and produced an apparent decrease in membrane resistance. The mean amplitude of G-1-induced depolarizations was concentration-dependent: G-1 (10 nM, 100 nM and 1 μM) depolarized

the nucleus ambiguus neurons by 2.3 ± 0.3 mV (n = 6), 12.1 ± 1.8 mV (n = 7) and 18.3 ± 0.8 mV (n = 3), respectively (Fig. 2E).

G-1 induced an inward current in nucleus ambiguus neurons in medullary slices

In voltage-clamp mode, the current-voltage relationship of neurons in response to voltage steps from −140 mV to 0 mV (Fig. 3A) was similar to that previously reported in nucleus ambiguus neurons (Mihalevich et al., 1996, Brailoiu et al., 2009). We examined the current-voltage (IV) relationships of membrane currents induced by G-1, in voltage-clamp mode. An example of IV relationship elicited by G-1 (100 nM) in nucleus ambiguus neurons is presented in Fig. 3B. Subtraction of the IV curves obtained before and during perfusion with G-1 revealed that G-1 induced an inward current (Fig. 3B-C).

Microinjection of G-1 to nucleus ambiguus in anesthetized rats elicited bradycardia

Baseline values for mean arterial pressure (MAP) and heart rate (HR) in urethane-anesthetized rats were 105.3 ± 8.14 mmHg and 415.3 ± 5.7 bpm (n = 5), respectively. Prior to performing microinjection of G-1 to the nucleus ambiguus, the location of nucleus ambiguus was functionally identified by the heart rate (HR) change following microinjection of L-glutamate (L-Glu). Microinjection of L-Glu (5 mM/30 nl) elicited a bradycardia with no concomitant change in blood pressure (n = 5), as previously reported (Chitravanshi and Sapru, 2011), indicating the correct placement of the micropipette in the nucleus ambiguus. The decrease in HR after the L-Glu microinjections was by 73.3 ± 7.5 bpm ($P < 0.001$); the values before and after the L-Glu were 416.3 ± 11.6 and 343 ± 11.1 bpm, respectively (Fig. 4A). Microinjection of G-1 (10 μM/30 nl), at the same site, elicited a decrease in HR with no concomitant change in blood pressure. Microinjection of G-1 (10 μM/30 nl) produced a decrease in HR by 59.7 ± 7.5 bpm ($p < 0.001$); the values before and after the G-1 were 430.6 ± 7.2 and 370 ± 9.1 bpm, respectively (n = 5) (Fig. 4A).

Reproducibility of G-1-induced responses

To test whether or not repetitive microinjection of G-1 produces tachyphylaxis, G-1, in the concentration that elicited bradycardic responses (10 μM/30 nl), was microinjected into the nucleus ambiguus at least 3 times, at 60 min intervals (n = 5). The decreases in HR induced by 3 consecutive microinjections of G-1 were 62.6 ± 2.2, 58 ± 1.4 and 60.8 ± 1.7 bpm, respectively ($P > 0.05$) (Fig. 3B). Thus, when the interval between injections was at least 60 min, repetitive microinjections of G-1 did not produce tachyphylaxis of bradycardic responses (Fig. 4B).

Microinjections of the GPER antagonist into nucleus ambiguus blocked the G-1-induced bradycardic responses

To further confirm the GPER specificity of the G-1-induced bradycardia, we tested the sensitivity of the response to treatment with GPER antagonist, G36 (Dennis et al., 2011). In these experiments (n = 5), the nucleus ambiguus was identified by microinjection of L-Glu (5 mM/30 nl) which elicited a decrease in heart rate by 72 ± 6.8 bpm without any change in BP (Fig 5A and 5B panel a). Microinjection of control vehicle (0.1% DMSO) into the same site, 5 min after L-Glu. did not elicit any significant change in BP and HR (Fig. 5B panel b). Microinjection of G-1 (10 μM/30 nl) into the same site of nucleus ambiguus produced a decrease in HR by 56.4 ± 2.7 bpm with no concomitant change in BP (Fig. 5A and 5B panel c). G-1 elicited a prolonged decrease in HR, with a duration of 25–30 min (Fig. 5B panel c). Sixty min later, microinjection of the GPCEr antagonist G-36 (10 μM/30 nl) into the same site did not elicited any significant changes in BP and HR (Fig. 5B panel d), but blocked the bradycardia induced by microinjection of G-1 (10 μM/30 nl) (Fig. 5B panel e). The decrease in HR produced by G-1 after G36 (10 μM/30 nl) was by only 4.6 ± 0.3 bpm ($P < 0.0001$) as

compared to 56.4 ± 2.7 bpm before the microinjection of the antagonist. The summarized group data is presented in Fig. 5A and a representative experiment is illustrated in Fig. 5B.

Site-specificity of G-1 responses

The bradycardic responses elicited from the nucleus ambiguus were site-specific because microinjections of G-1 (10 μM/30 nl) into the adjacent areas (e.g., ventral region of the dorsal medullary reticular nucleus; 0.6 mm rostral and 2.3 mm lateral to the CS and 2.6 mm deep from the dorsal medullary surface) elicited no HR responses (n = 5). The HR values before and after the G-1 into the above adjacent area were 408.4 ± 9.3 and 404 ± 9.2 bpm, respectively ($P > 0.05$).

Histological identification of microinjection sites

Composite diagrams of the microinjection sites (n = 10) in the nucleus ambiguus, where microinjections of L-Glu and G-1 elicited bradycardia are presented in Fig. 6A–E; each dot corresponds to one rat.

Intravenous injection of G-1 produces bradycardia

G-1 (41.2 ng/kg to 20.6 μg/kg, iv) in addition to a previously reported decrease in blood pressure (Haas et al., 2009), produced a concentration-dependent decrease in the HR. Intravenous injection of G-1 (41.2 ng/kg, 412 ng/kg, 4.12 μg/kg and 20.6 μg/kg) reduced the heart rate by 0.8 ± 0.3 % (n = 5), 4.8 ± 0.8 % (n = 7), 7.5 ± 0.7 % (n = 8) and 8.3 ± 0.8 % (n = 7), respectively (Fig. 7A). The bradycardic effect induced by G-1 (4.12 μg/kg) was prevented by i.v. injection of atropine (2 mg/kg) (n = 5), a potent muscarinic receptor antagonist (Fig. 7A).

Bilateral microinjections of G36 into the nucleus ambiguus blocked the bradycardia induced by systemic injection of G-1

Intravenous (i.v.) injection of G-1 (4.12 μg/kg) decreased MAP by 10 ± 3.1 mmHg and HR (33 ± 9.9 bpm; 7.7 %) (n = 5); a representative example is shown in Fig. 7B (panel a). Sixty min after the recovery of blood pressure and HR to basal values, the left and right nucleus ambiguus were identified by microinjection of L-Glu (5 mM/30 nl), which elicited a bradycardia (60 ± 7.9 bpm) without any changes in MAP (Fig. 7B, panel b), as previously reported (Chitravanshi & Sapru, 2011). Five min later, microinjection of control vehicle (Veh, 0.1% DMSO) into the same site did not elicit any changes in HR and MAP (Fig. 7B panel c). G-36 (10 μM/30 nl), a GPER antagonist, was bilaterally microinjected into the nucleus ambiguus five min after the injection of control vehicle; the injection of G36 did not elicit any change in BP and HR (Fig. 7B panel d). G-1 (4.12 μg/kg) i.v. injected 5 min after the microinjection of the antagonist produced a markedly reduced change in HR (Fig. 7B panel e) (3.8 ± 3.1 bpm; $p < 0.05$) whereas the decrease in MAP was not significantly affected ($p > 0.05$). Control microinjection of L-Glu (5 mM/30 nl) after the GPER blockade with G36 elicited bradycardia (Fig. 7B panel f).

Discussion

Increasing evidence supports a role for GPER in estrogen-mediated fast signaling (Prossnitz and Barton, 2011). While most of our knowledge is derived from studies of GPER in breast and ovarian cancers and cell lines, the physiologic role of this novel receptor is just beginning to unravel (Olde and Leeb-Lundberg, 2009). Activation of GPER has been involved in modulation of physiological functions in the nervous, cardiovascular, reproductive, endocrine, and immune systems (Prossnitz and Barton, 2011). In the context of this study, the identification of GPER immunoreactivity in cholinergic neurons of the

nucleus ambiguus (Brailoiu et al., 2007), a medullary site critical for the autonomic cardiovascular regulation, provided the impetus to evaluate the role of GPER in the modulation of the vagal tone to the heart. This is particularly important as the modulation of the autonomic tone seems to contribute to the cardiovascular protective effects of estrogen (Du et al., 1995, Liu et al., 2003).

Using calcium and voltage imaging, we first evaluated the effects of GPER activation in cardiac vagal neurons of nucleus ambiguus retrogradely labeled with rhodamine. GPER activation has been shown to mobilize Ca^{2+} in several cell types (Revankar et al., 2005, Bologa et al., 2006, Brailoiu et al., 2007; Filardo et al., 2007; Noel et al., 2009; Dennis et al. 2011; Tica et al., 2011; Deliu et al., 2012). In cultured cardiac vagal neurons, administration of G-1 produced a concentration-dependent increase in cytosolic Ca^{2+}. The response was GPER-specific, as pretreatment with the recently identified GPER antagonist G36 (Dennis et al., 2011), prevented the G-1-induced Ca^{2+} increase. A transitory increase in Ca^{2+} is a common signaling pathway in neurons (Berridge, 1998); it may lead to cellular depolarization. Indeed, voltage imaging experiments indicate that G-1 depolarized cardiac vagal neurons via a GPER-dependent mechanism.

Using classical electrophysiological techniques, we also examined the effect of G-1 on nucleus ambiguus neurons in a brainstem slice preparation. In a rat medullary slice, the nucleus ambiguus can be easily identified as a cluster of cells in the rostroventrolateral medulla area (Bouairi et al., 2006; Brailoiu et al., 2009, 2012). Whole-cell patch-clamp recordings in current clamp mode indicate that G-1 produced a dose-dependent depolarization. At higher concentration tested (100 nM and 1000 nM), G-1-induced depolarization was accompanied by a decrease in membrane resistance, indicating an increase in membrane conductance. Voltage-clamp recordings support this finding, as GPER activation induced an inward current. Similarly, previous reports showed that GPER activation depolarized spinal cord neurons (Dun et al., 2009, Deliu et al., 2012), restored excitability in vagal neurons from ovariectomized rats (Qiao et al., 2009), or had a rapid excitatory effect on primate LHRH neurons (Noel et al., 2009).

Similar to the nuclear estrogen receptors (Vanderhorst et al., 2005), no significant gender differences were reported in the CNS distribution of GPER between male and female rats (Brailoiu et al., 2007); however a sexually dimorphic distribution was found in the hamster brain (Canonaco et al., 2008). GPER expression levels in rat hippocampus, were not different among adults male and female in proestrus or estrus (Matsuda et al., 2008). Despite a partial overlap with ERα or ERβ mRNA in different regions, GPR30 immunoreactivity in the rat brain was identified in cell populations distinct from those expressing ERα and ERβ within many brain nuclei (Brailoiu et al., 2007), while colocalized in others (Spary et al., 2009). The levels of expression of ERs in the rat CNS appear to change over the oestrus cycle in response to these fluctuations in circulating oestrogen (Spary et al., 2009). Moreover, previous reports indicate circadian and estrous cycle-dependent variations in blood pressure and heart rate in female rats (Takezawa et al., 1994). In the present study, to avoid any response variability due to fluctuations in estrogen levels in female rats, during the estrous cycle, only adult male rats were used in *in vivo* experiments.

In vivo recordings of heart rate and blood pressure in anesthetized adult male rats indicate that G-1 microinjected into the nucleus ambiguus decreased the heart rate, without affecting the blood pressure; the effect was blocked by pretreatment with the GPER antagonist, G36 (Dennis et al., 2011). Previous reports indicate that central administration of estrogen in cardiovascular and autonomic medullary nuclei of male and ovariectomized female rats significantly increased the baroreflex function and vagal nerve activity in male and ovariectomized female rats (Saleh and Connell, 1999; Saleh et al., 2000a, b). The increase in

phenylephrine-induced bradycardic response started 5 min after estrogen administration and reached a peak 30 min after the injection. Similarly, in the present work, G-1 injected into the nucleus ambiguus produced a decrease in heart rate that lasted 25–30 min. Earlier receptor profiling for G-1, conducted at 10 μM, indicates that G-1 does not bind to the human M1, M2 and M3 muscarinic receptors, expressed in Sf9 insect cells (Blasko et al., 2009). We therefore do not expect any direct effect of G-1 on rat muscarinic receptors.

Intravenous injection of G-1, in addition to the previously reported reduction in blood pressure (Haas et al., 2009), produced a concentration-dependent decrease in heart rate. In the absence of a direct effect of G-1 on heart rate regulation, the G-1-induced decrease in blood pressure would have elicited a compensatory increase in heart rate via baroreflex. The reduction in heart rate produced by G-1 further supports a direct activation of nucleus ambiguus neurons, as indicated by the microinjection studies. Moreover, atropine prevented G-1-induced bradycardia, indicating the involvement of muscarinic receptors in the response. In addition, the bradycardic effect of systemic administration of G-1 was blocked by microinjection of GPER antagonist in the nucleus ambiguus, further supporting nucleus ambiguus as a site of GPER-mediated bradycardia. The blood pressure lowering effect of G-1 is most likely due to the vasodilation reported in several arterial beds (Haas et al., 2009; Meyer et al., 2010, Broughton et al., 2010, Yu et al., 2011). Both endothelium-dependent (Broughton et al., 2010) and endothelium–independent mechanisms (Yu et al., 2011) have been identified.

As GPER-expressing neurons of the nucleus ambiguus have a cholinergic phenotype (Brailoiu et al., 2007), our results support the hypothesis that GPER activation in nucleus ambiguus neurons stimulates the release of acetylcholine in cardiac vagal terminals, which in turn decreases the heart rate. This is also supported by the fact that intravenous administration of G-1 decreased heart rate, which was abolished by atropine.

Notable differences in effective concentrations of GPER ligands were reported in different cellular systems and between endogenously expressing and GPER-transfected cells; these may be due to the differences in the number or availability of the receptors and/or different downstream signaling mechanisms involved. Published reports, including ours, indicate that in primary cells, G-1 activates GPER in the high nanomolar to micromolar range (Brailoiu et al., 2007; Maiti et al., 2011; Tica et al., 2011; Deliu et al., 2012). In transfected cells, which overexpress the receptor, lower concentrations of agonists were sufficient to activate the receptor (Revankar et al., 2005).

Taken together our results indicate a novel role for GPER in increasing cardiac parasympathetic tone, thereby effectively slowing the heart, which may be cardioprotective. A direct, cardioprotective role of GPER activation has been also reported in a rat ischemic model (Deschamps et al., 2009).

Acknowledgments

This study was supported by NIH grants HL090804 (EB) and CA127731 (TIO, JBA) from the Department of Health and Human Services. We thank Dr. Nae J. Dun for the review of an earlier version of the manuscript.

References

Blasko E, Haskell CA, Leung S, Gualtieri G, Halks-Miller M, Mahmoudi M, Dennis MK, Prossnitz ER, Karpus WJ, Horuk R. Beneficial role of the GPR30 agonist G-1 in an animal model of multiple sclerosis. J Neuroimmunol. 2009; 214:67–77. [PubMed: 19664827]

Berridge MJ. Neuronal calcium signaling. Neuron. 1998; 21:13–26. [PubMed: 9697848]

Bologa CG, Revankar CM, Young SM, Edwards BS, Arterburn JB, Kiselyov AS, Parker MA, Tkachenko SE, Savchuck NP, Sklar LA, Oprea TI, Prossnitz ER. Virtual and biomolecular screening converge on a selective agonist for GPR30. Nat Chem Biol. 2006; 2:207–212. [PubMed: 16520733]

Bouairi E, Kamendi H, Wang X, Gorini C, Mendelowitz D. Multiple types of GABAA receptors mediate inhibition in brain stem parasympathetic cardiac neurons in the nucleus ambiguus. J Neurophysiol. 2006; 96:3266–3272. [PubMed: 16914614]

Brailoiu E, Dun SL, Brailoiu GC, Mizuo K, Sklar LA, Oprea TI, Prossnitz ER, Dun NJ. Distribution and characterization of estrogen receptor G protein-coupled receptor 30 in the rat central nervous system. J Endocrinol. 2007; 193:311–321. [PubMed: 17470522]

Brailoiu E, Hooper R, Cai X, Brailoiu GC, Keebler MV, Dun NJ, Marchant JS, Patel S. An ancestral deuterostome family of two-pore channels mediates nicotinic acid adenine dinucleotide phosphate-dependent calcium release from acidic organelles. J Biol Chem. 2010a; 285:2897–2901. [PubMed: 19940116]

Brailoiu GC, Brailoiu E, Chang JK, Dun NJ. Excitatory effects of human immunodeficiency virus 1 Tat on cultured rat cerebral cortical neurons. Neuroscience. 2008; 151:701–710. [PubMed: 18164555]

Brailoiu GC, Brailoiu E, Parkesh R, Galione A, Churchill GC, Patel S, Dun NJ. NAADP-mediated channel ‘chatter’ in neurons of the rat medulla oblongata. Biochem J. 2009; 419:91–97. 92. following 97. [PubMed: 19090786]

Brailoiu GC, Gurzu B, Gao X, Parkesh R, Aley PK, Trifa DI, Galione A, Dun NJ, Madesh M, Patel S, Churchill GC, Brailoiu E. Acidic NAADP-sensitive calcium stores in the endothelium: agonist-specific recruitment and role in regulating blood pressure. J Biol Chem. 2010b; 285:37133–37137. [PubMed: 20876534]

Brailoiu GC, Deliu E, Tica AA, Chitravanshi VC, Brailoiu E. Urocortin 3 elevates cytosolic calcium in nucleus ambiguus neurons. J Neurochem. 2012; 122:1129–1136. [PubMed: 22774996]

Brauner T, Hulser DF, Strasser RJ. Comparative measurements of membrane potentials with microelectrodes and voltage-sensitive dyes. Biochim Biophys Acta. 1984; 771:208–216. [PubMed: 6704395]

Broughton BR, Miller AA, Sobey CG. Endothelium-dependent relaxation by G protein-coupled receptor 30 agonists in rat carotid arteries. Am J Physiol Heart Circ Physiol. 2010; 298:H1055–1061. [PubMed: 20061543]

Canonaco M, Giusi G, Madeo A, Facciolo RM, Lappano R, Canonaco A, Maggiolini M. A sexually dimorphic distribution pattern of the novel estrogen receptor G-protein-coupled receptor 30 in some brain areas of the hamster. J Endocrinol. 2008; 196:131–138. [PubMed: 18180324]

Chitravanshi VC, Sapru HN. Microinjections of urocortin1 into the nucleus ambiguus of the rat elicit bradycardia. Am J Physiol Heart Circ Physiol. 2011; 300:H223–229. [PubMed: 20952663]

Dart AM, Du XJ, Kingwell BA. Gender, sex hormones and autonomic nervous control of the cardiovascular system. Cardiovasc Res. 2002; 53:678–687. [PubMed: 11861039]

Deliu E, Brailoiu GC, Arterburn JB, Oprea TI, Benamar K, Dun NJ, Brailoiu E. Mechanisms of G protein-coupled estrogen receptor-mediated spinal nociception. J Pain. 2012; 13:742–754. [PubMed: 22858342]

Dennis MK, Field AS, Burai R, Ramesh C, Petrie WK, Bologa CG, Oprea TI, Yamaguchi Y, Hayashi S, Sklar LA, Hathaway HJ, Arterburn JB, Prossnitz ER. Identification of a GPER/GPR30 antagonist with improved estrogen receptor counterselectivity. J Steroid Biochem Mol Biol. 2011; 127:358–366. [PubMed: 21782022]

Deschamps AM, Murphy E. Activation of a novel estrogen receptor, GPER, is cardioprotective in male and female rats. Am J Physiol Heart Circ Physiol. 2009; 297:H1806–1813. [PubMed: 19717735]

Du XJ, Riemersma RA, Dart AM. Cardiovascular protection by oestrogen is partly mediated through modulation of autonomic nervous function. Cardiovasc Res. 1995; 30:161–165. [PubMed: 7585800]

Dun SL, Brailoiu GC, Gao X, Brailoiu E, Arterburn JB, Prossnitz ER, Oprea TI, Dun NJ. Expression of estrogen receptor GPR30 in the rat spinal cord and in autonomic and sensory ganglia. J Neurosci Res. 2009; 87:1610–1619. [PubMed: 19125412]

Ebner TJ, Chen G. Use of voltage-sensitive dyes and optical recordings in the central nervous system. Prog Neurobiol. 1995; 46:463–506. [PubMed: 8532849]

Filardo E, Quinn J, Pang Y, Graeber C, Shaw S, Dong J, Thomas P. Activation of the novel estrogen receptor G protein-coupled receptor 30 (GPR30) at the plasma membrane. Endocrinology. 2007; 148:3236–3245. [PubMed: 17379646]

Grynkiewicz G, Poenie M, Tsien RY. A new generation of Ca2+ indicators with greatly improved fluorescence properties. J Biol Chem. 1985; 260:3440–3450. [PubMed: 3838314]

Haas E, Bhattacharya I, Brailoiu E, Damjanovic M, Brailoiu GC, Gao X, Mueller-Guerre L, Marjon NA, Gut A, Minotti R, Meyer MR, Amann K, Ammann E, Perez-Dominguez A, Genoni M, Clegg DJ, Dun NJ, Resta TC, Prossnitz ER, Barton M. Regulatory role of G protein-coupled estrogen receptor for vascular function and obesity. Circ Res. 2009; 104:288–291. [PubMed: 19179659]

Huikuri HV, Pikkujamsa SM, Airaksinen KE, Ikaheimo MJ, Rantala AO, Kauma H, Lilja M, Kesaniemi YA. Sex-related differences in autonomic modulation of heart rate in middle-aged subjects. Circulation. 1996; 94:122–125. [PubMed: 8674168]

Liu CC, Kuo TB, Yang CC. Effects of estrogen on gender-related autonomic differences in humans. Am J Physiol Heart Circ Physiol. 2003; 285:H2188–2193. [PubMed: 12881217]

Maiti K, Paul JW, Read M, Chan EC, Riley SC, Nahar P, Smith R. G-1-activated membrane estrogen receptors mediate increased contractility of the human myometrium. Endocrinology. 2011; 152:2448–2455. [PubMed: 21427217]

Matsuda K, Sakamoto H, Mori H, Hosokawa K, Kawamura A, Itose M, Nishi M, Prossnitz ER, Kawata M. Expression and intracellular distribution of the G protein-coupled receptor 30 in rat hippocampal formation. Neurosci Lett. 2008; 441:94–99. [PubMed: 18586395]

Mendelowitz D. Firing properties of identified parasympathetic cardiac neurons in nucleus ambiguus. Am J Physiol. 1996; 271:H2609–2614. [PubMed: 8997322]

Mendelowitz D. Advances in Parasympathetic Control of Heart Rate and Cardiac Function. News Physiol Sci. 1999; 14:155–161. [PubMed: 11390842]

Mercuro G, Podda A, Pitzalis L, Zoncu S, Mascia M, Melis GB, Rosano GM. Evidence of a role of endogenous estrogen in the modulation of autonomic nervous system. Am J Cardiol. 2000; 85:787–789. A789. [PubMed: 12000064]

Meyer MR, Baretella O, Prossnitz ER, Barton M. Dilation of epicardial coronary arteries by the G protein-coupled estrogen receptor agonists G-1 and ICI 182,780. Pharmacology. 2010; 86:58–64. [PubMed: 20639684]

Mihalevich M, Neff RA, Mendelowitz D. Voltage-gated currents in identified parasympathetic cardiac neurons in the nucleus ambiguus. Brain Res. 1996; 739:258–262. [PubMed: 8955946]

Mohamed MK, El-Mas MM, Abdel-Rahman AA. Estrogen enhancement of baroreflex sensitivity is centrally mediated. Am J Physiol. 1999; 276:R1030–1037. [PubMed: 10198382]

Noel SD, Keen KL, Baumann DI, Filardo EJ, Terasawa E. Involvement of G protein-coupled receptor 30 (GPR30) in rapid action of estrogen in primate LHRH neurons. Mol Endocrinol. 2009; 23:349–359. [PubMed: 19131510]

Olde B, Leeb-Lundberg LM. GPR30/GPER1: searching for a role in estrogen physiology. Trends Endocrinol Metab. 2009; 20:409–416. [PubMed: 19734054]

Prossnitz ER, Barton M. The G-protein-coupled estrogen receptor GPER in health and disease. Nat Rev Endocrinol. 2011; 7:715–726. [PubMed: 21844907]

Paxinos, G.; Watson, C. The rat brain in stereotaxic coordinates. Academic Press; San Diego, CA: 1998.

Qiao GF, Li BY, Lu YJ, Fu YL, Schild JH. 17Beta-estradiol restores excitability of a sexually dimorphic subset of myelinated vagal afferents in ovariectomized rats. Am J Physiol Cell Physiol. 2009; 297:C654–664. [PubMed: 19570896]

Revankar CM, Cimino DF, Sklar LA, Arterburn JB, Prossnitz ER. A transmembrane intracellular estrogen receptor mediates rapid cell signaling. Science. 2005; 307:1625–1630. [PubMed: 15705806]

Saleh MC, Connell BJ, Saleh TM. Medullary and intrathecal injections of 17beta-estradiol in male rats. Brain Res. 2000a; 867:200–209. [PubMed: 10837814]

Saleh MC, Connell BJ, Saleh TM. Autonomic and cardiovascular reflex responses to central estrogen injection in ovariectomized female rats. Brain Res. 2000b; 879:105–114. [PubMed: 11011011]

Saleh TM, Connell BJ. Centrally mediated effect of 17beta-estradiol on parasympathetic tone in male rats. Am J Physiol. 1999; 276:R474–481. [PubMed: 9950927]

Saleh TM, Connell BJ. 17beta-estradiol modulates baroreflex sensitivity and autonomic tone of female rats. J Auton Nerv Syst. 2000; 80:148–161. [PubMed: 10785281]

Saleh TM, Connell BJ. Role of oestrogen in the central regulation of autonomic function. Clin Exp Pharmacol Physiol. 2007; 34:827–832. [PubMed: 17645624]

Spary EJ, Maqbool A, Batten TF. Oestrogen receptors in the central nervous system and evidence for their role in the control of cardiovascular function. J Chem Neuroanat. 2009; 38:185–196. [PubMed: 19505570]

Takezawa H, Hayashi H, Sano H, Saito H, Ebihara S. Circadian and estrous cycle-dependent variations in blood pressure and heart rate in female rats. Am J Physiol. 1994; 267:R1250–1256. [PubMed: 7977852]

Tica AA, Dun EC, Tica OS, Gao X, Arterburn JB, Brailoiu GC, Oprea TI, Brailoiu E. G protein-coupled estrogen receptor 1-mediated effects in the rat myometrium. Am J Physiol Cell Physiol. 2011; 301:C1262–1269. [PubMed: 21865584]

Vanderhorst VG, Gustafsson JA, Ulfhake B. Estrogen receptor-alpha and -beta immunoreactive neurons in the brainstem and spinal cord of male and female mice: relationships to monoaminergic, cholinergic, and spinal projection systems. J Comp Neurol. 2005; 488:152–179. [PubMed: 15924341]

Virtanen I, Polo O, Polo-Kantola P, Kuusela T, Ekholm E. The effect of estrogen replacement therapy on cardiac autonomic regulation. Maturitas. 2000; 37:45–51. [PubMed: 11099873]

Weissman A, Lowenstein L, Tal J, Ohel G, Calderon I, Lightman A. Modulation of heart rate variability by estrogen in young women undergoing induction of ovulation. Eur J Appl Physiol. 2009; 105:381–386. [PubMed: 18989692]

Yu X, Ma H, Barman SA, Liu AT, Sellers M, Stallone JN, Prossnitz ER, White RE, Han G. Activation of G protein-coupled estrogen receptor induces endothelium-independent relaxation of coronary artery smooth muscle. Am J Physiol Endocrinol Metab. 2011; 301:E882–888. [PubMed: 21791623]

New Findings

1. What is the current scientific knowledge on this specific topic?

Background to this study

Clinical and experimental studies indicate that estrogen increases cardiac vagal tone. The role of the G protein-coupled estrogen receptor (GPER) in the autonomic cardiac control is not known.

2. What New Findings does this research study add to this field?

What this study adds

Using calcium imaging and electrophysiological techniques and *in vivo* studies, microinjection in nucleus ambiguus and measurement of cardiovascular responses, we show that activation of GPER in cardiac vagal neurons of the nucleus ambiguus increases cytosolic Ca^{2+} and depolarizes these neurons, leading to a decrease in heart rate. Our findings suggest a novel role for GPER in cardiac vagal tone modulation.

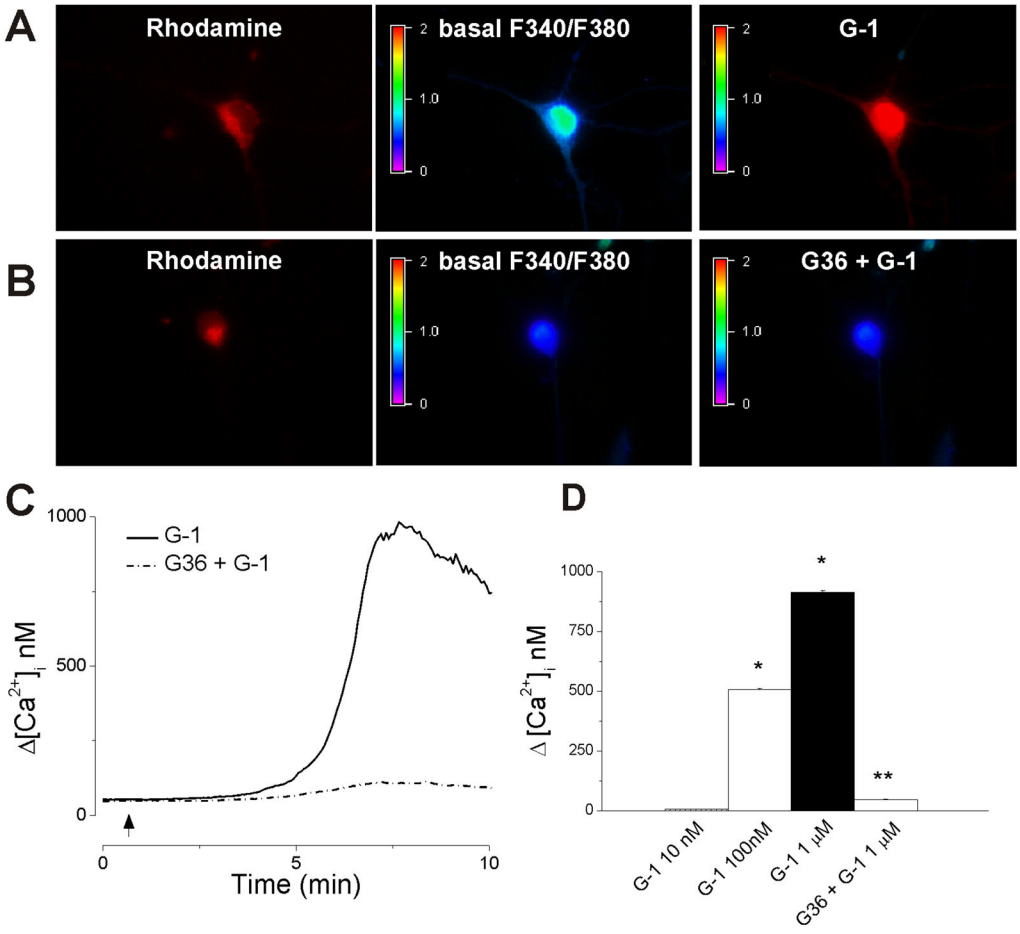

Fig. 1. Activation of GPER in cardiac vagal neurons of nucleus ambiguus increases cytosolic Ca^{2+}

A, Illustration of Fura-2 AM fluorescence ratio (F340/F380 nm) before (basal) and after G-1 treatment in cardiac preganglionic vagal neurons of nucleus ambiguus retrogradely labeled with rhodamine. B, Pretreatment with G36 prevented the increase in F340/F380 ratio produced by G-1. C, Representative recordings of cytosolic Ca^{2+} concentration, $[Ca^{2+}]_i$ in response to G-1 in the absence (solid trace) and presence (dotted trace) of the GPER antagonist, G36. D, Comparison of increases in cytosolic Ca^{2+} concentration ($\Delta[Ca^{2+}]_i$) produced by different concentrations of G-1 (10 nM - 1 μM) in the absence and presence of G36 (1 μM). *, $P < 0.05$ as compared to basal $[Ca^{2+}]_i$; **, $P < 0.05$, as compared to the increase in $[Ca^{2+}]_i$ produced by G-1 (1μM).

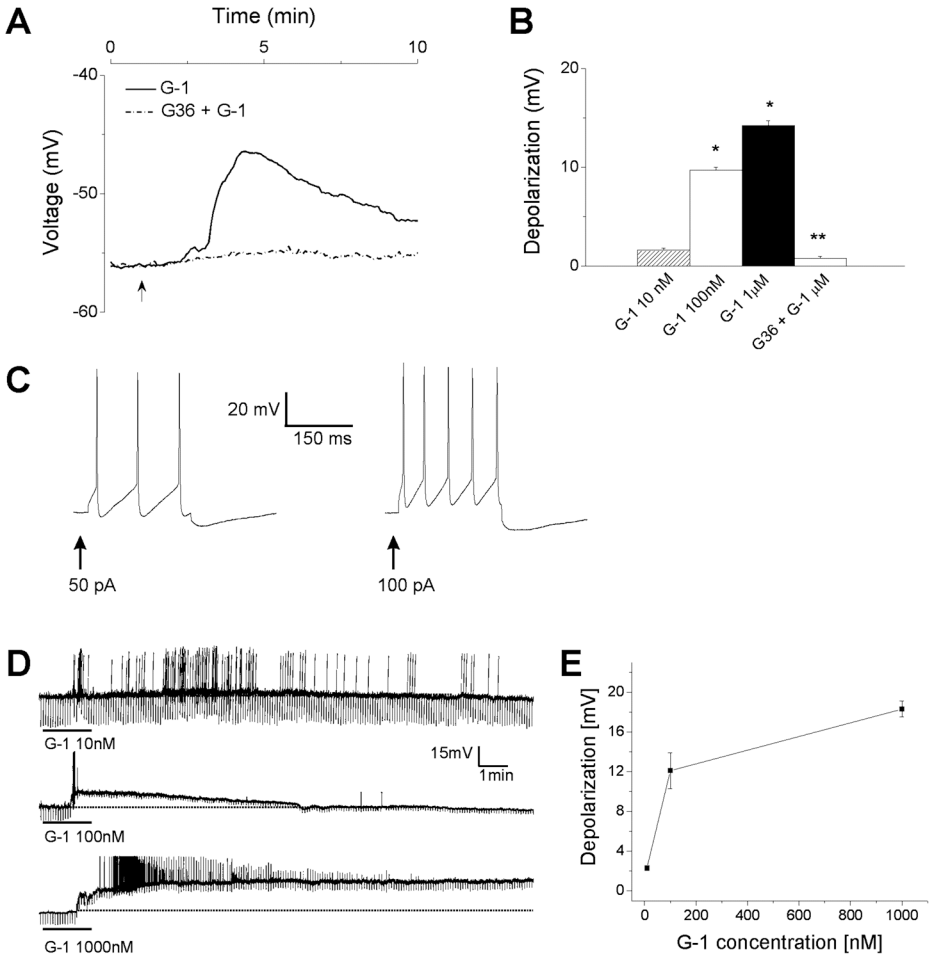

Fig. 2. G-1-induced depolarization of nucleus ambiguus neurons

A, Representative example of G-1-induced depolarization (solid trace) in cultured retrogradely labeled cardiac vagal neurons of nucleus ambiguus; the effect was prevented by pretreatment with G36 (dotted trace). B, Comparison of the mean amplitude of depolarizations produced by G-1 (10 nM - 1 μM) in the absence and presence of G36 (1 μM) in retrogradely labeled cardiac vagal neurons. *, $P < 0.05$ as compared to resting membrane potential; **, $P < 0.05$, as compared to the depolarization produced by G-1 (1μM). C, Electrophysiological properties of nucleus ambiguus neurons in medullary slices. Depolarizing stimuli (50 pA and 100 pA) elicited action potentials. D, G-1 (10 nM, 100 nM and 1000 nM) caused an increase in firing activity and depolarization accompanied by a decrease in membrane resistance. Downward deflections superimposed on the membrane potential are hyperpolarizing electrotonic potentials induced by constant current pulses (30 pA amplitude, 300 ms duration), and were used to monitor the membrane resistance. E, G-1 (10 nM – 1000 nM) produced a concentration-dependent depolarization.

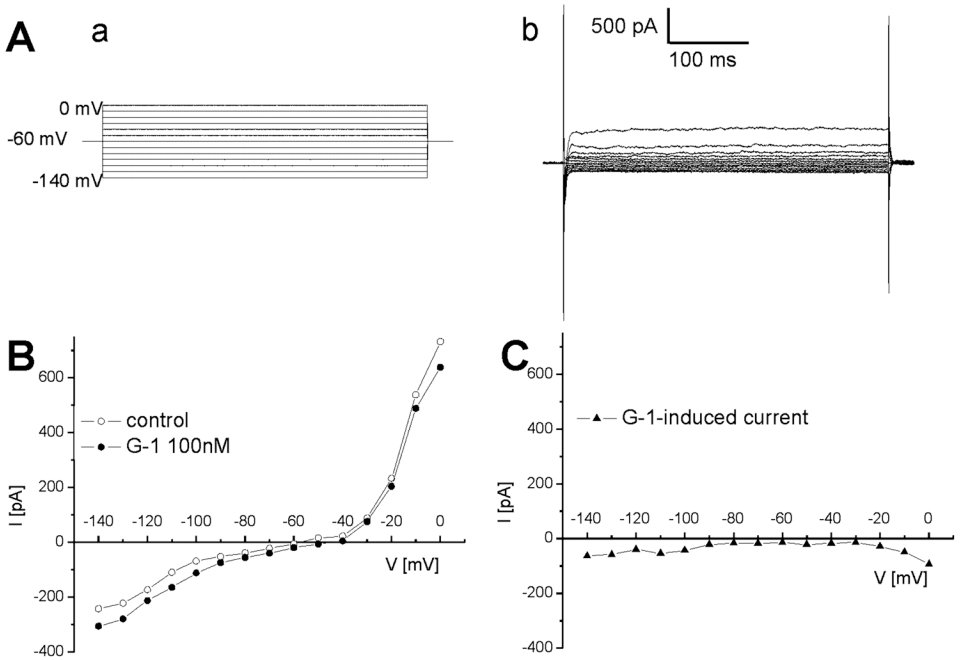

Fig. 3. G-1-induced inward current in nucleus ambiguus neurons

A, Voltage steps (a) from −140 to 0 mV applied from a holding current of −60 mV induced currents (b) whose steady state values were used to construct current-voltage relationships. B, Representative example of steady state current values in response to voltage steps from −140 to 0 mV, before and after administration of G-1 (100 nM). C, Representative example of G-1-induced inward currents obtained by substraction of the IV curves obtained before and during perfusion with G-1.

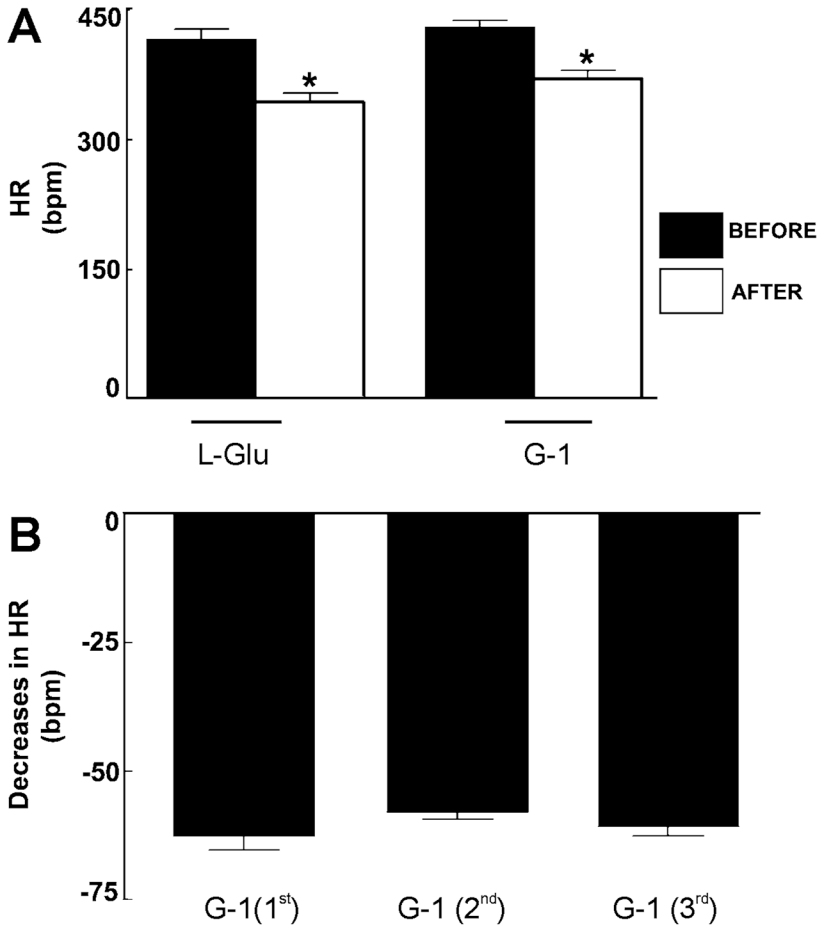

Fig. 4. Bar diagrams showing decreases in heart rate elicited by microinjection of L-Glu and G-1 into the nucleus ambiguus

A, Comparison of heart rate (HR) values before and after microinjection of L-Glu (5 mM/30 nl) and G-1 (10 μM/30 nl) into the nucleus ambiguus. * $P < 0.001$. B, Decreases in HR elicited by three consecutive microinjections of G-1 (10 μM/30 nl); no tachyphylaxis was seen with repeated microinjections of G-1 when the interval was kept at least 60 min.

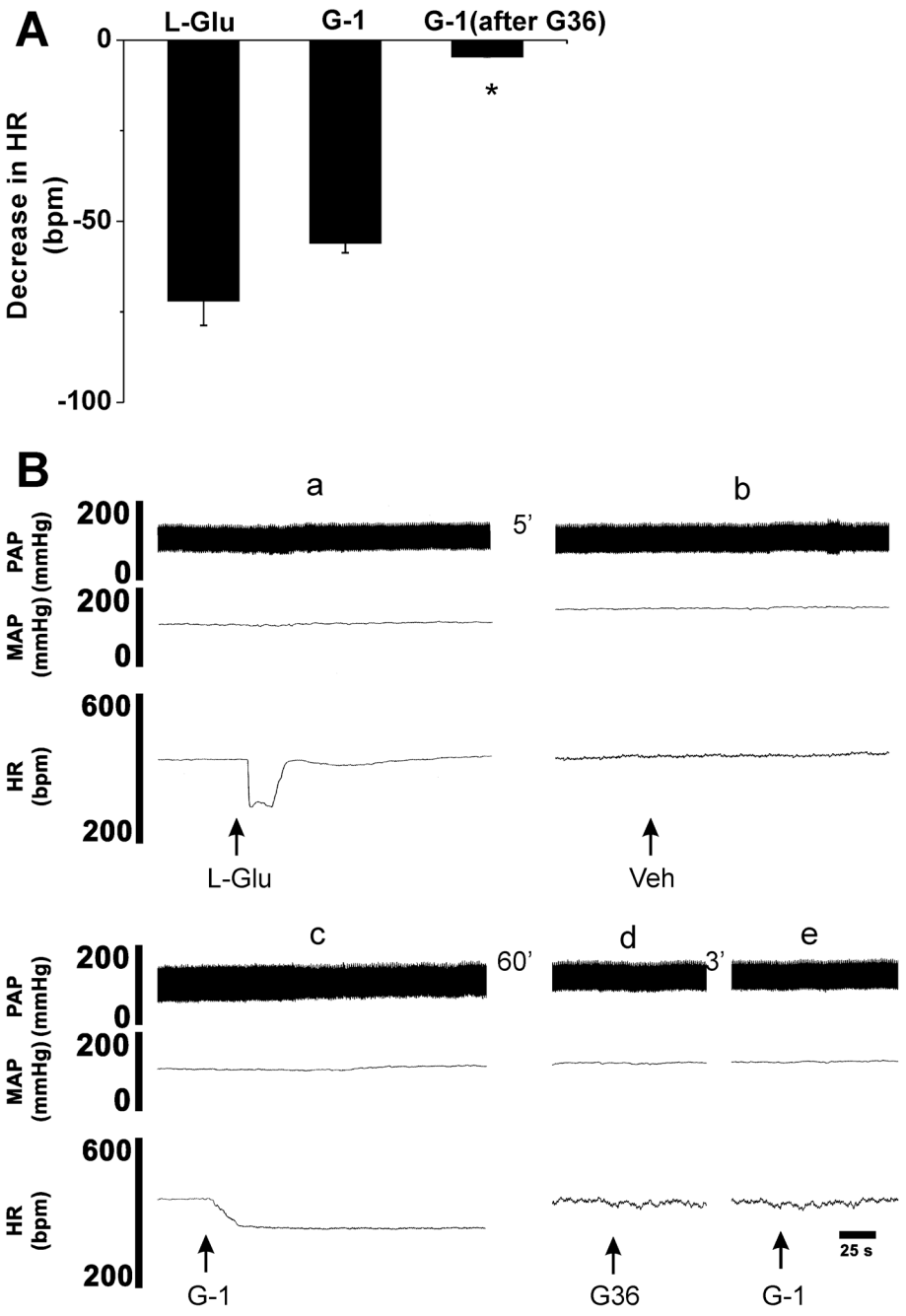

Fig. 5. Blockade of G-1 induced bradycardia by prior microinjections of the GPER antagonist

A, Group data summarizing the decrease in heart rate (HR) produced by microinjection of L-Glu (5 mM/30 nl), G-1 (10 μM/30 nl) and G-1 (10 μM/30 nl) after the antagonist, G36 (10 μM/30 nl), into the nucleus ambiguus (*$P < 0.0001$ as compared to G-1 microinjection before G36). B, Illustration of a representative experiment, where injection of L-glutamate (L-Glu, 5 mM,/30 nl) into nucleus ambiguus elicited a bradycardia (a). At the same site, microinjection of vehicle (Veh, DMSO 0.1%) did not elicit any changes in heart rate (HR) or blood pressure (b). Microinjection of G-1 (10 μM/30 nl) at the same site elicited a prolonged bradycardia with no changes in blood pressure (c). Microinjection of G-36 (10 μM/30 nl) into nucleus ambiguus did not change the HR and blood pressure (d), but blocked

the G-1-induced bradycardia (e). Abbreviations: MAP, mean arterial pressure, PAP, pulsatile arterial pressure.

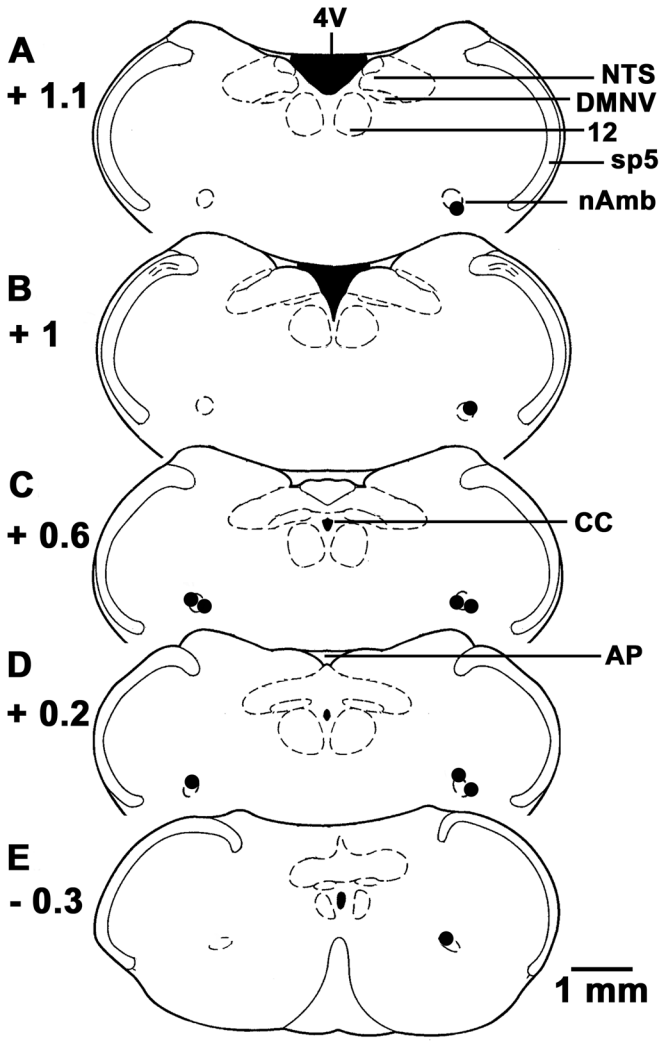

Fig. 6. Histological identification of microinjection sites

A–E, Drawings of coronal sections at levels 1.1 mm rostral to 0.3 mm caudal to the calamus scriptorius (CS). Microinjection sites are shown as dark spots; each spot represents a site in one animal (n = 10). Abbreviations: AP, area postrema; CC, central canal; DMNV, dorsal motor nucleus of vagus; nAmb, nucleus ambiguus; NTS, nucleus tractus solitarius; Sp5, spinal trigeminal tract; 4V, fourth ventricle; 12, hypoglossal nucleus.

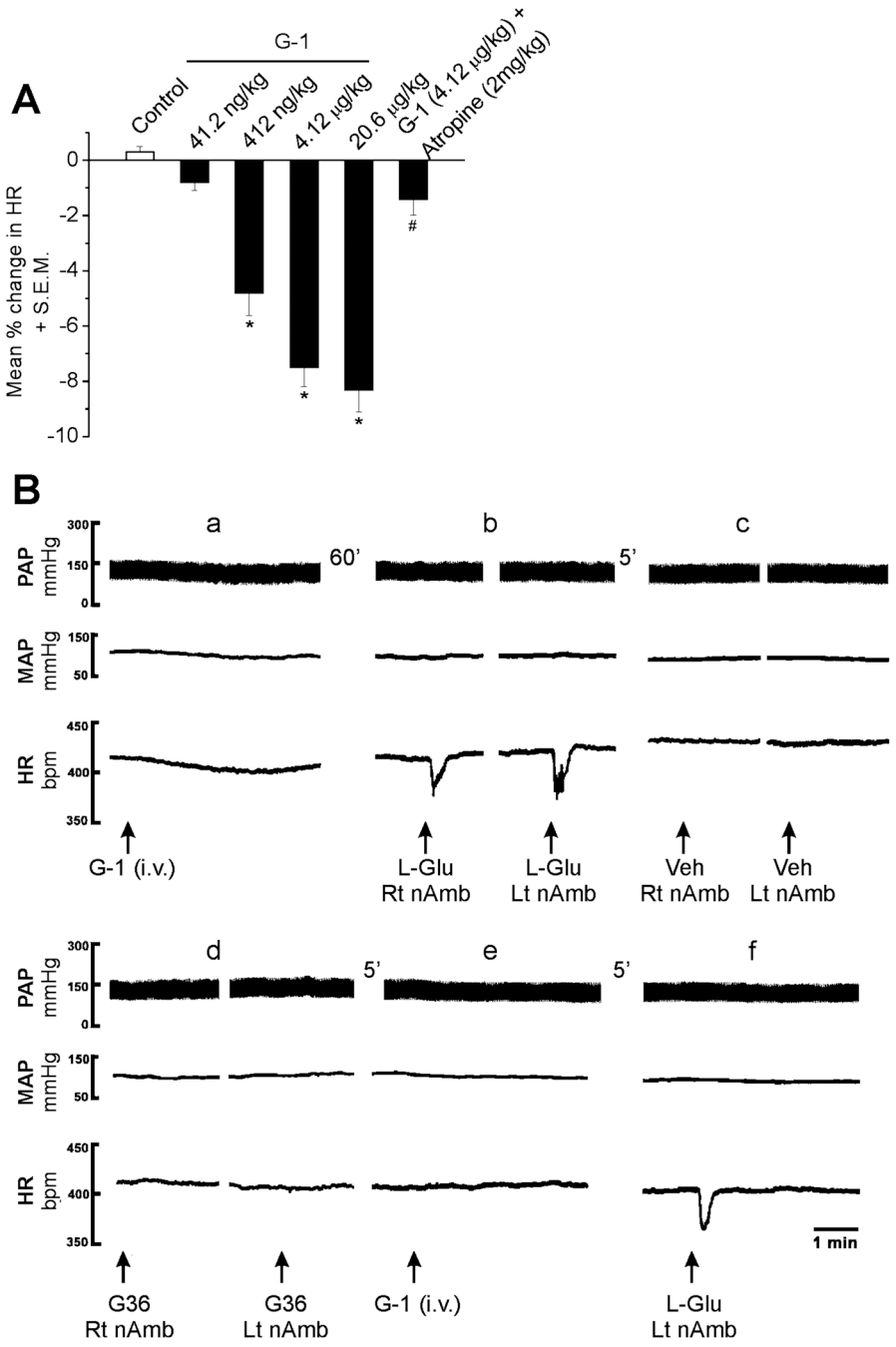

Fig. 7. Bilateral microinjections of G36 into the nucleus ambiguous blocked the bradycardia induced by systemic injection of G-1

A, G-1 (41.2 ng/kg – 20.6 μg/kg) produced a concentration-dependent decrease in HR; the bradycardia induced by G-1 (4.12 μg/kg) was markedly decreased by atropine (2 mg/kg) *, $P < 0.05$ as compared to control saline injection; #, P<0.05 as compared to G-1 (4.12 μg/kg). **B**, Systemic (i.v.) administration of G-1 (4.12 μg/kg) elicited a decrease in heart rate and blood pressure (a). Bilateral microinjection of L-Glu (5 mM/30 nl) into the nucleus ambiguus, 60 min later, elicited bradycardia without any changes in blood pressure (b), while bilateral microinjection of vehicle (Veh, 0.1% DMSO) into the same site did not elicit any changes in BP and HR (c). Bilateral microinjection of G36 did not have any effect on

HR and blood pressure by itself (d), but blocked the G-1-induced bradycardia (e). The L-Glu-induced bradycardia was preserved after GPER blockade (f). Abbreviations: HR, heart rate; MAP, mean arterial pressure, PAP, pulsatile arterial pressure; Lt nAmb, left nucleus ambiguus, and Rt nAmb, right nucleus ambiguus.